Electronic and transport properties of carbon nanotube peapods

A. Rochefort
École Polytechnique de Montréal, Département de génie physique, Montréal, (Qué) Canada H3C 3A7
and CERCA, Groupe Nanostructures, Montréal, (Qué) Canada H3X 2H9
(Received 30 September 2002; published 5 March 2003)

We theoretically studied the electronic and electrical properties of metallic and semiconducting nanotube peapods with encapsulated C_{60} (C_{60}@CNT) as a function of the carbon nanotube (CNT) diameter. For exothermic peapods (the CNT diameter$>$11.8 Å), only minor changes, ascribed to a small structural deformation of the nanotube walls, were observed. These include a small electron charge transfer (less than 0.10 electron) from the CNT to the C_{60} molecules and a poor mixing of the C_{60} orbitals with those of the CNT. Decreasing the diameter of the nanotube leads to a modest increase of the charge density located between the C_{60}'s. More significant changes are obtained for endothermic peapods (CNT diameter$<$11.8 Å). We observe a large electron charge transfer from C_{60} to the tube, and a drastic change in electron transport characteristics and electronic structure. These results are discussed in terms of π-π interaction and C_{60} symmetry breaking.

DOI: 10.1103/PhysRevB.67.115401 PACS number(s): 73.23.−b, 73.50.−h, 73.20.At, 73.61.Wp

I. INTRODUCTION

The possibility of using new forms of carbon-based materials for practical applications in nanoelectronics has stimulated an important amount of exciting works during the last decade.[1] Since their discovery in 1991, carbon nanotubes (CNTs) have been used as an active component in the fabrication of transistor,[2–4] memory elements,[5] and more recently, logic circuits.[6,7] CNTs can also be used as a template for nanofabrication and as reservoirs for the storage of gas, ions, or metals.[8] In this respect, it was recently shown experimentally that multiple C_{60} molecules can penetrate into a carbon nanotube to form a one-dimensional array of C_{60} nested inside.[9] This type of carbon materials, due to its original structure, is often called a carbon peapod.

Filling CNTs with C_{60} is exothermic or endothermic depending on the size of the nanotube.[10] C_{60}@(10,10) was found to be stable (exothermic) while other peapods with a smaller CNT shell such as the (9,9) and (8,8) tubes are endothermic. Metallic CNTs preserve most of their intrinsic properties upon the encapsulation of C_{60} molecules. The interaction between C_{60} and the nanotube occurs through a weak orbital mixing between a near-free-electron state on the CNT located above Fermi level (and most probably above vacuum level) and the *p* orbitals of the C_{60}. This interaction leads to a weak electron confinement between C_{60} and the CNT wall, and a slight charge transfer from the tube to the C_{60}. Therefore, only little perturbation is expected. However, recent scanning tunneling microscopy results showed a drastic modification of the local electronic structure of semiconducting nanotube peapods.[11] This perturbation is essentially present in the conduction band. The main variation observed is a sharp increase in the density of states (DOS) probed directly over an encapsulated C_{60} molecule. This increase in the DOS was tentatively attributed to the electronic coupling of C_{60} with the CNT shell, which is estimated approximately to about 1 eV.[11] This tube-C_{60} coupling appears much stronger than anticipated by theory[10] or experimental work on metallic peapods.[12] It is therefore important to study further the properties of encapsulated C_{60} on the electrical and electronic properties of both metallic and semiconducting nanotubes as a function of the nanotube diameter. In the present study, we show that the electronic as well as electron transport properties of exothermic peapods do not show drastic differences from the properties of individual species. The CNT-C_{60} interaction increases slightly as the nanotube diameter decreases, but becomes very important for endothermic peapods.

II. COMPUTATIONAL DETAILS

We considered the encapsulation of up to three C_{60} molecules in approximately 10-nm-long metallic and semiconductor CNT models containing up to 1500 carbon atoms. The C_{60} molecules were systematically placed in the middle sections of the CNT. The region where C_{60}'s are encapsulated is relatively small with respect to the entire CNT length, thus avoiding the influence of the open boundary conditions implicit to our finite model. The computed stabilization energy (ΔE_S) corresponds to the energy difference between a fully optimized peapod structure and the isolated species (perfect CNT and isolated C_{60}'s). Prior to the optimization, the dangling bonds at both ends of the finite nanotube models were saturated with hydrogen. The activation energy needed to introduce the C_{60}'s in the CNT was not evaluated. Stabilization energies were calculated with the MM3 molecular mechanic force field[13] (the bond parameter of alkene was modified to 1.42 Å) and the geometries were optimized with a standard conjugated gradient technique down to a root mean square (rms) deviation $<10^{-5}$. We previously showed that this modified-MM3 force field gives a total energy that is in good agreement with the more accurate tight-binding density-functional theory (DFT) method.[14] The electronic structure calculations for the CNT and peapod systems were carried out within the extended Hückel (EH) method, which includes an explicit treatment of overlap integral for the *s* and *p* valence orbital of carbon.[15] It has been shown that the EH method gives results similar to those obtained on extended CNTs with more sophisticated methods.[16]

The electrical transport properties of carbon nanotubes

and peapods were computed using a Green's function approach[17] within the Landauer-Büttiker formalism. The Hamiltonian and overlap matrices used in this formalism were also determined using the EH model.[15] For transport calculations, the two ends of the CNT were bonded to gold electrodes. The metallic contacts consist of a sufficient number of gold atoms in a (111) crystalline arrangement to create a larger contact area relative to the CNT ends. In order to minimize the contact resistance, the distance between the gold pad and the tube end was fixed to 1.5 Å.[14] The Green's function of the conductor can be written in the form of block matrices explicitly separating the molecular Hamiltonian,

$$G_C=[E\mathcal{S}_C-\mathcal{H}_C-\Sigma_1-\Sigma_2]^{-1}, \quad (1)$$

where $\mathcal{S}_C$ and $\mathcal{H}_C$ are the overlap and the Hamiltonian matrices of the conductor (nanotube or peapod), respectively, and $\Sigma_{1,2}$ are self-energy terms describing the effect of the leads. The transmission function $\overline{T}(E)$ (or transmittance), which is the summation of transmission probabilities over all conduction channels in the system, is obtained from the Green's function of the conductor (G_C) given by[17]

$$\overline{T}(E)=\overline{T}_{21}=\mathrm{Tr}[\Gamma_2 G_C \Gamma_1 G_C^{\dagger}]. \quad (2)$$

In this formula, the matrices have the form

$$\Gamma_{1,2}=i(\Sigma_{1,2}-\Sigma_{1,2}^{\dagger}). \quad (3)$$

III. RESULTS AND DISCUSSION

The existence of encapsulated C_{60} inside a CNT can be discussed in term of a stabilization energy (ΔE_S) in the form of

$$\Delta E_S \equiv E[x\mathrm{C}_{60}@(n,m)]-E[(n,m)]-xE[C_{60}],$$

where x is the number of C_{60} molecules, and (n,m) is the chirality index of the nanotube considered. The variation of the stabilization energy as a function of the nanotube diameter (D_{NT}) for a single encapsulated C_{60} molecule is shown in Fig. 1, while Table I gives ΔE_S (reported by C_{60}) values for multiple encapsulated C_{60} molecules. In order to qualitatively describe the influence of the π-electron cloud on the resulting peapods stability, we show an additional curve (the dotted line) in Fig. 1, where the thickness of the π cloud ($\approx$3.3 Å) is subtracted from the nanotube diameters. The stabilization energy for peapods with a large diameter CNT shell is relatively weak and exothermic. On the other hand, C_{60} can more easily penetrate into a large CNT because the interaction energy is weak. As the CNT diameter decreases, the interaction energy between the C_{60} molecule and the CNT wall becomes more important; the ΔE_S values then reflect the balance between van der Waals attraction and Coulomb repulsion. The most stable peapod is the $x\mathrm{C}_{60}@(10,10)$ system, in which the π-electron clouds of both C_{60} and CNT just begin to overlap. For a CNT smaller than the (10,10) tube, the peapods become rapidly less stable and highly endothermic (i.e., positive ΔE_S) at D_{NT} $<$11.9 Å. The range of tube diameters where peapods are the most stable ($12<D_{NT}<15$ Å) is in good agreement with

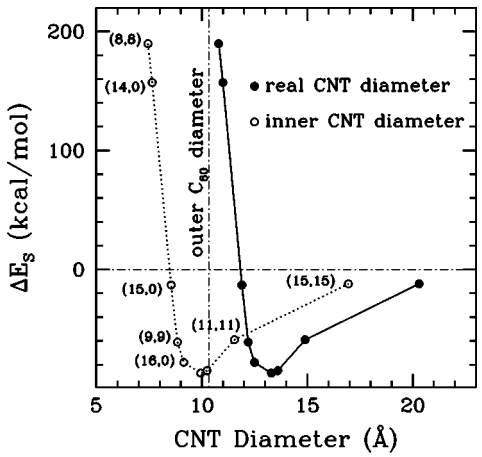

FIG. 1. Stabilization energy ΔE_S for the introduction of a C_{60} molecule into a 100-Å-long carbon nanotube (H-terminated). Inner and outer diameter is when we considere the thickness of the π-electron cloud. Exothermic peapods have negative ΔE_S, and endothermic peapods have positive values.

recent experimental[18] and theoretical[10,19] observations. The $C_{60}@(9,9)$ peapod was previously found[10] slightly endothermic (by 6 kcal/mol) with the DFT method. The lower stability found for $C_{60}@(9,9)$ with DFT is probably related to the imposed commensurate structure of the C_{60} within the tube in their supercell model. The relative stability of small peapods is strongly related to the ability of the tube to satisfy the presence of encapsulated C_{60} molecules through a deformation of its structure, especially near the C_{60} molecules. As expected, the smaller the CNT, the larger the structural deformations, and consequently lower is the stability of the peapod.[10,19] This also reflects on the C_{60}-C_{60} distance ($d_{C_{60}\text{-}C_{60}}$); C_{60} molecules in small CNTs become squashed, and the distance between their centers increases (see Table I). In the following, we first compare the electronic and electrical properties of the most stable metallic $[C_{60}@(10,10)]$ and semiconducting $[C_{60}@(16,0)]$ peapods. Then we present the results for the highly endothermic $C_{60}@(14,0)$ peapod.

Figure 2 compares the DOS of perfect-CNT/peapod systems (upper panels), and the local density of states (LDOS) of the CNT shell of these peapods (lower panels) in a region near the C_{60}, for the (A) metallic $3C_{60}@(10,10)$ and (B) semiconducting $3C_{60}@(16,0)$ structures. The vertical dotted-dashed lines indicate the energy position where a difference in LDOS was observed between a perfect CNT and a peapod for which the contribution of the C_{60} molecules was removed. This last comparison allows us to highlight the changes induced by a structural deformation rather than by an electronic influence of C_{60} on the CNT. The finite DOS at the Fermi energy (E_F) for $C_{60}@(10,10)$, and the absence of states at E_F for the $C_{60}@(16,0)$ peapod, suggest that the fundamental (metal, semiconductor) electronic characteristics of the CNTs are preserved upon C_{60} encapsulation. The presence of C_{60} in the peapods clearly results in additional peaks in the DOS for valence and conduction bands of both metallic and semiconducting peapods. The first two peaks near E_F, associated with C_{60} are observed at around -1.0 and

TABLE I. Variation of the carbon peapods properties as a function of the nanotube diameter.

Peapod type	CNT diameter (Å)	$d_{C60\text{-}C60}$ [a] (Å)	Mulliken charge (e/C_{60})	$\Delta E_S/C_{60}$ (kcal/mol)
C_{60}@(15,15)	20.3	-	−0.00	−12
C_{60}@(10,10)	13.7	-	−0.02	−85
$2C_{60}$@(10,10)		9.7	−0.02	−89
$3C_{60}$@(10,10)		9.7	−0.02	−90
C_{60}@(16,0)	12.5	-	−0.07	−78
$2C_{60}$@(16,0)		9.8	−0.08	−81
$3C_{60}$@(16,0)		9.8	−0.08	−83
C_{60}@(9,9)	12.2	-	−0.14	−61
C_{60}@(15,0)	11.9	-	−0.03	−13
C_{60}@(14,0)	11.1	-	+1.59	157
$2C_{60}$@(14,0)		10.1	+1.59	155
$3C_{60}$@(14,0)		10.1	+1.59	155
C_{60}@(8,8)	10.8	-	+1.44	190

[a]Distance between the center of adjacent C_{60}.

+0.2 eV for $3C_{60}$@(10,10), and at around −0.7 and +0.5 eV for $3C_{60}$@(16,0). These peaks correspond respectively to the highest-occupied HOMO and lowest unoccupied molecular orbital (HOMO and LUMO) of C_{60}. The calculated HOMO-LUMO gap (1.2 eV) for encapsulated C_{60} is smaller than the value calculated for isolated C_{60} (1.6 eV), and the experimental values (≈1.6–1.8 eV) for C_{60} in gas and solid phases.[20] This difference is partly related to the deformation of C_{60} which contributes to closing the gap of C_{60},[22] and to the displacement of C_{60} orbitals induced by the relatively weak interaction between C_{60} and the CNT. In addition, the very small charge transfer[21] from the CNT to the C_{60} molecule (see Table I), and the weak mixing of states between C_{60} and the CNT (C_{60} states are weakly spread in

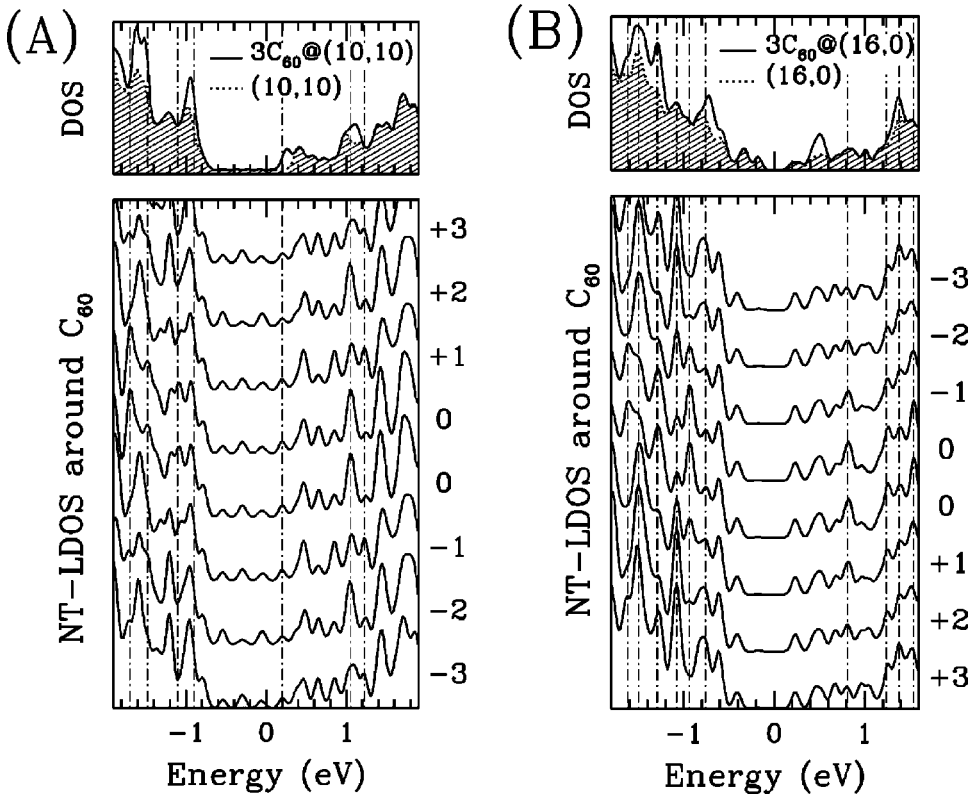

FIG. 2. Density of states (DOS) and local density of states (LDOS) of (A) metallic (10,10) and (B) semiconducting (16,0) nanotubes and peapods. DOS (upper panels) compares perfect (streaked line) and C_{60} filled tubes (full line), while LDOS (lower panels) shows the contribution of a circular section of carbon atoms in the vicinity of a C_{60} molecule (0 is directly over C_{60}, and ±1, ±2 is gradually away from C_{60}).

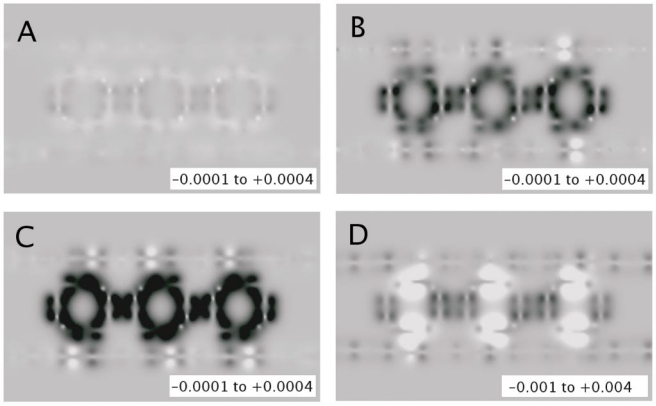

FIG. 3. Representation of the residual valence charge density of the $3C_{60}@(n,m)$ peapods where (A) $n=m=10$, (B) $n=16,m=0$, (C) $n=m=9$, and (D) $n=14,m=0$. A negative value in the scale corresponds to a loss of charge density (bright region) while a positive indicates a gain of charge density (dark region). A similar scale is kept from (A) to (C) to emphasize the effect of the tube diameter on the charge density, and the scale for (D) is an order of magnitude higher.

the DOS for peapods) support that only weak interaction between C_{60} and the nanotube wall are present. This result is in agreement with previous DFT description of metallic peapods, in which a very weak charge transfer was observed.[10] The influence of the CNT diameter on the charge density distribution is represented in Fig. 3, in which we consider the residual charge density ρ_r such as

$$\rho_r=\rho[x\mathrm{C}_{60}@(n,m)]-\rho[x\mathrm{C}_{60}]-\rho[(n,m)],$$

and where the dark and bright regions indicate a gain and loss of the electron charge density, respectively. As the CNT diameter decreases, the accumulation of the charge density between the C_{60} molecules, and between the C_{60} and the CNT shell increases, leaving the C_{60} molecules slightly more negative than the isolated species. This result contrasts slightly with previous DFT results, where the weak accumulation of negative charge density in large diameter peapods was mainly located in the space between the tube and C_{60}.[10] This charge density localization, which is practically absent for peapods smaller than the (10,10) tube, was attributed to the presence of a weak coupling between C_{60} and a near free electron state of the CNT, which is known to be poorly described within the EH method. The case of a $C_{60}@(14,0)$ peapod (*D*) is quite different. There is an important loss of charge density between the C_{60} and the CNT shell and a small gain of charge density between C_{60}'s. As discussed below, this behavior is mainly related to C_{60} symmetry breaking.

The LDOS of peapods (lower panels of Fig. 2) also suggests a weak influence of the C_{60} molecules on the electronic properties of the CNT peapods. In these LDOS diagrams, the label "0" marks the carbons that are the closest to C_{60}, and the labels $\pm1, \pm2, \ldots$ are for carbon sections progressively away from the central "0" position. For the metallic $3C_{60}@(10,10)$ peapod [see Fig. 2(A)], the most important changes occur in the valence band between -1.7 and -1.1 eV. These variations are more directly related to the states created by structural deformation of the CNT shell (indicated by the vertical dash-dotted lines) as opposed to the possible electronic influence of C_{60}. A similar situation occurs for the semiconducting $3C_{60}@(16,0)$ peapod, except that a smaller tube diameter results in slightly higher electronic influence on the LDOS of the (16,0) tube. A certain number of structurally deformed states (dash-dotted lines) coincide with the

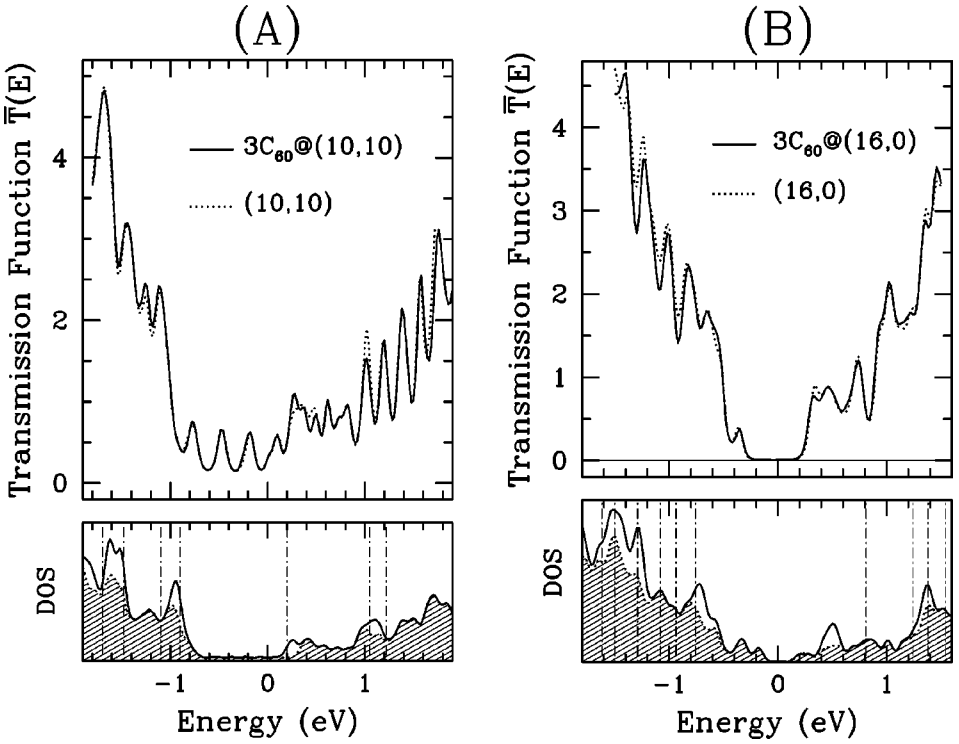

FIG. 4. Variation of the electron transport (upper panels) and electronic (lower panels) properties from (n,m) to $3C_{60}@(n,m)$ systems, for (A) $n=m=10$ and (B) $n=16$, $m=0$. The electronic structure of a perfect (n,m) tube (lower panels) is indicated by the dotted line-streaked area.

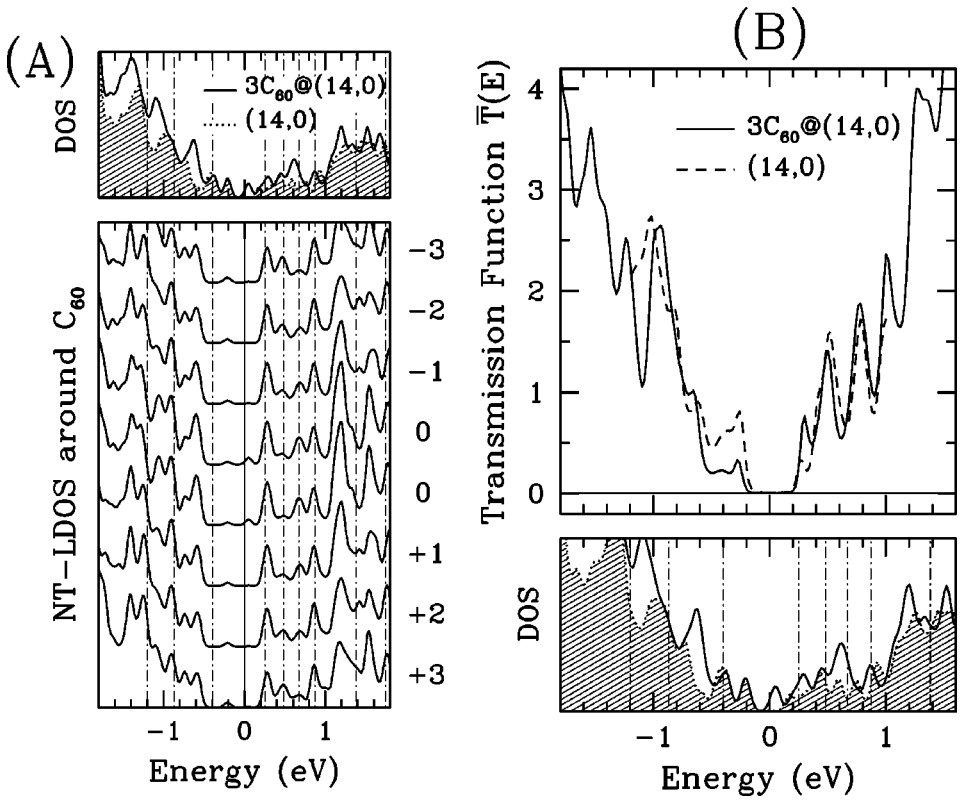

FIG. 5. Comparison of electronic structure (A) and electrical (B) properties between the (14,0) and the $3C_{60}$@(14,0) systems.

presence of C_{60} states, and suggest a possible mixing of states. In contrast to the DOS where the contributions of the tube and the three C_{60} molecules are convoluted, the local variation of DOS in the vicinity of a single C_{60} remains almost imperceptible. This result is in strong constrast with previous scanning tunneling microscopy (STM) measurements in which a very important increase of LDOS was observed but only for the conduction band of a semiconducting peapod.[11] The slight variations in valence and conduction bands observed in the present study for semiconducting (and metallic) peapods suggest that an additionnal phenomenom could occur in the STM experiment, and may explain the discrepancy. For example, a Coulomb blockade event or a structural deformation of carbon peapod induced by the STM tip can alter significantly the spectroscopic signature. There is clearly a possible blockade in that the charging energy of C_{60} exceeds 270 meV, which is much larger than kT.[23]

The transport properties of the (A) metallic (10,10) and (B) semiconducting (16,0) nanotubes are not very much altered by the encapsulation of C_{60}'s. The main panels of Fig. 4 shows the variation of the transmission function $\overline{T}(E)$ (or transmittance) for perfect and C_{60} filled nanotubes as a function of electron energy. We also reproduce the DOS curves of CNTs and peapods (lower panels) in Fig. 4 to identify the energy position where changes are observed. For the metallic tube, the presence of transmittance peaks, instead of a plateau, near E_F is mainly due to our finite model for which the bands still have a molecular (discrete) character. The imperfect gold-CNT contact induces an extra contact resistance (of ≈ 8 kΩ) to the minimal resistance of 6 kΩ for a metallic (ballistic) nanotube, and lowers the transmittance at E_F from 2 to ≈ 0.8.[24] However, since the CNTs and peapods have similar gold-tube geometries, we are expecting a similar contact resistance. The regions where small changes in transmittance are observed agree well with the features observed in the DOS associated with C_{60} [see Fig. 4(A)]. As observed for the electronic structure properties, the small diameter of the (16,0) tube facilitates a slight improvement of orbital mixing between the CNT and the C_{60}'s. As a result, the transport properties of the (16,0) tube are more altered than for the (10,10) tube, especially in the valence band. However, these changes remain quite weak, and suggest that it would be experimentally very difficult to differentiate between a perfect nanotube and a peapod, at least on the basis on their electronic and electrical properties.

The existence of the highly endothermic C_{60}@(14,0) peapod is highly improbable because of the large activation energy needed for encapsulation (see Table I). This highly deformed peapod is however quite rich in information. The structure of C_{60}@(14,0) contains a bumped CNT shell near C_{60}'s. Because of the small inner space in a (14,0) tube, the C_{60} molecules are significantly squashed into an elliptic shape. Figure 5 shows the variation of the electronic (A) and electrical (B) properties between a perfect (14,0) tube and a $3C_{60}$@(14,0) peapod. The DOS and LDOS diagrams (left panels) of the peapod show drastic variations with respect to the perfect (14,0) tube, more specifically in the band-gap region where low energy bound states appear for the peapod. The influence of C_{60} can now be clearly identified in the LDOS curves over a large range of energy in both valence and conduction band. In addition, as the vertical dash-dotted lines indicate, the variation of the electronic structure of the (14,0) tube is mostly induced by structural deformations. This is deduced from a comparison of the perfect (14,0) tube

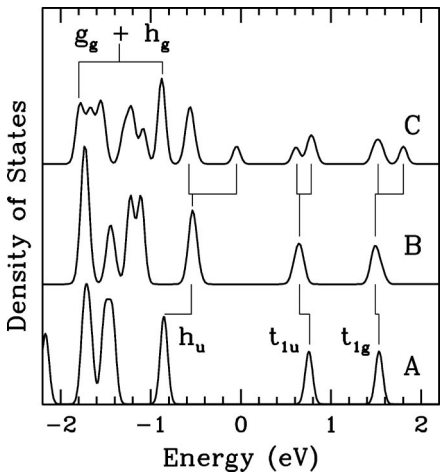

FIG. 6. Effect of space (tube) diameter on the electronic structure of (A) free C_{60} when encapsulated in (B) (10,10), and (B) (14,0) CNTs. Vertical lines show the origins and the displacement of splitted orbitals induce by symmetry breaking.

and the empty peapod system. Considering the large charge transfer from C_{60} to the tube [see Table I and Fig. 3(D)], it is clear that C_{60} has an important electronic and structural effect on the (14,0) tube properties in a peapod. This influence reflects on the transport properties where important fluctuations of the transmittance are observed near the first band edge of the conduction and valence bands. Nevertheless, the change of transmittance at E_F is very weak and only a small difference is observed between the perfect tube and the peapod. Although we do not want to emphasize the electronic and transport properties of this endothermic peapod, the electronic structure of the squashed C_{60} in this $3C_{60}$@(14,0) peapod is useful to gain insight about the nature of the charge transfer involved in peapods.

In Fig. 6, we compare the electronic structure of three different geometries of a C_{60} triad, one with a ideal C_{60} geometry (A), a second with the C_{60} structure as in the (10,10) tube (B), and a third with the compressed C_{60} structure as in the (14,0) tube (C). The symmetry group of the orbitals and their corresponding positions in the different arrangements are also included. The fivefold-degenerate h_u and threefold-degenerate t_{1u} bands correspond to the HOMO and LUMO, respectively. Except for the small displacement of the HOMO and LUMO orbitals, and the small symmetry breaking of the $g_g + h_g$ manifold band at higher binding energy, the electronic structure of encapsulated-like C_{60} molecules as in (10,10), is very similar to free C_{60}. On the other hand, the symmetry breaking of C_{60} orbitals is very significant for the compressed geometry as in the C_{60}@(14,0) peapod. The more important band splitting is about the HOMO (h_u) where the symmetry breaking produces one fourfold-degenerate band, and an isolated orbital that is strongly shifted toward E_F. This type of band splitting was already predicted for a single C_{60} molecule by Joachim *et al.*[22] The presence of an occupied orbital near E_F of the peapod significantly increases the ability of C_{60} to donate electrons. In addition, as observed in LDOS of $3C_{60}$@(14,0) peapod (see Fig. 5), the low-lying energy states in the band gap of the (14,0) tube related to the regions of deformed CNTs, are placed in the appropriate range of energies to receive an extra electron from C_{60}. A charge transfer from the low-lying orbital of squashed C_{60} near E_F to the tube would then explain the important loss of charge density on the C_{60} molecules observed near the nanotube wall reported in Table I, and the large net positive charge on C_{60} for the $3C_{60}$@(14,0).

In summary, the electronic and electrical properties of metallic and semiconducting carbon nanotubes for the most stable carbon peapods are not significantly altered by the encapsulation of C_{60}. Only a weak charge transfer is observed from the nanotube wall to the C_{60} molecules. This change, mostly located between C_{60}, supports a weak orbital mixing between the two species. As the nanotube diameter decreases, within the exothermic peapods limit, a small increase in the charge transfer and orbital mixing is observed. For the case of endothermic peapods, the changes in electronic and electrical properties are very drastic. The most important and relevant effect remains the C_{60} symmetry breaking that induces the splitting of the HOMO (h_u band) into several components, especially one near E_F. This effect improves the electron donation ability of C_{60} in the peapods.

ACKNOWLEDGMENTS

I am grateful to RQCHP for providing computational resources. I am also pleased to acknowledge Richard Martel for his comments and for helpful discussions, and Patrick Desjardins for his comments on the manuscript.

[1] M. S. Dresselhaus, G. Dresselhaus, and Ph. Avouris, *Carbon Nanotubes: Synthesis, Structure, Properties, and Applications* (Springer-Verlag, Berlin, 2001).
[2] S. J. Tans, A. R. M. Verschueren, and C. Dekker, Nature (London) **393**, 49 (1998).
[3] R. Martel, T. Schmidt, H. R. Shea, T. Hertel, and Ph. Avouris, Appl. Phys. Lett. **73**, 2447 (1998).
[4] H. W. Ch. Postma, T. Teepen, Z. Yao, M. Grifoni, and C. Dekker, Science **293**, 76 (2001).
[5] T. Rueckes, K. Kim, E. Joselevich, G. Y. Tseng, C.-L. Cheung, and C. M. Lieber, Science **289**, 94 (2000).
[6] V. Derycke, R. Martel, J. Appenzeller, and Ph. Avouris, Nano. Lett. **1**, 453 (2001).
[7] A. Bachtold, P. Hadley, T. Nakanishi, and C. Dekker, Science **294**, 1317 (2001).
[8] J. Sloan, J. Hammer, M. Zwiefka-Sibley, and M. L. Green, Chem. Commun. (Cambridge) **3**, 347 (1998).
[9] B. W. Smith, M. Monthioux, and D. E. Luzzi, Nature (London) **396**, 323 (1998); B. W. Smith and D. E. Luzzi, Chem. Phys. Lett. **321**, 169 (2000).
[10] S. Okada S. Saito, and A. Oshiyama, Phys. Rev. Lett. **86**, 3835 (2001).

[11] D. J. Hornbaker, S.-J. Kahng, S. Misra, B. W. Smith, A. T. Johnson, E. J. Mele, D. E. Luzzi, and A. Yazdani, Science **295**, 828 (2002).
[12] X. Liu, T. Pichler, M. Knupfer, M. S. Golden, J. Fink, H. Kataura, Y. Achiba, K. Hirahara, and S. Iijima, Phys. Rev. B **65**, 045419 (2002).
[13] N. L. Allinger, Y. H. Yuh, and J.-H. Lii, J. Am. Chem. Soc. **111**, 8551 (1989).
[14] A. Rochefort, Ph. Avouris, F. Lesage, and D. R. Salahub, Phys. Rev. B **60**, 13 824 (1999).
[15] G. Landrum, *YAeHMOP* (Yet Another Extended Hückel Molecular Orbital Package), Cornell University, Ithaca, NY, 1995.
[16] A. Rochefort, D. R. Salahub, and Ph. Avouris, J. Phys. Chem. B **103**, 641 (1999).
[17] S. Datta, *Electronic Transport in Mesoscopic Systems* (Cambridge University Press, Cambridge, UK, 1995).
[18] S. Bandow, M. Takizawa, K. Hirahara, M. Yudasaka, and S. Iijima, Chem. Phys. Lett. **337**, 48 (2001).
[19] D. Qian, W. K. Liu, and R. S. Ruoff, J. Phys. Chem. B **105**, 10753 (2001).
[20] M. S. Dresselhaus, G. Dresselhaus, and P. C. Eklund, *Science of Fullerenes and Carbon Nanotubes* (Academic, San Diego, 1996).
[21] The net charge was evaluated from a Mulliken analysis of the extended Hückel (EH) calculations. We are not pretending to determine a quantitative charge distribution within EH theory, even if the present description of a charge transfer is qualitatively correct.
[22] C. Joachim, J. K. Gimzewski, and H. Tang, Phys. Rev. B **58**, 16407 (1998).
[23] H. Park, J. Park, A. K. L. Lim, E. H. Anderson, A. P. Alivisatos, and P. L. McEuen, Nature (London) **407**, 57 (2000).
[24] The extra resistance of gold-nanotube contacts depends on the structural compatibility between the Au(111) crystal and the carbon atoms in the circular section which is the diameter. An extra-resistance of 5 kΩ was found for a (6,6) tube in Ref. 14.